Proton Spin Diffusion in Polyethylene as a Function of Magic-Angle Spinning Rate. A Phenomenological Approach

ARTICLE *in* THE JOURNAL OF PHYSICAL CHEMISTRY A · MARCH 2008

Impact Factor: 2.69 · DOI: 10.1021/jp077067u · Source: PubMed

4 AUTHORS, INCLUDING:

Qun Chen
Central South University
180 PUBLICATIONS **1,313** CITATIONS
SEE PROFILE

Eddy Walther. Hansen
University of Oslo
112 PUBLICATIONS **1,467** CITATIONS
SEE PROFILE

Proton Spin Diffusion in Polyethylene as a Function of Magic-Angle Spinning Rate. A Phenomenological Approach

Zhenlong Jia,[†] Lili Zhang,*[,‡] Qun Chen,*[,†] and E. W. Hansen*[,‡]

Physics Department and the State Key Laboratory of Precision Spectroscopy Laboratory for Optics and Magnetic Resonance Spectroscopy, East China Normal University, 3663 Northern Zhongshan Road, Shanghai 200062, People's Republic of China, and University of Oslo, Department of Chemistry, P.O. Box 1033 Blindern, N-0315 Oslo, Norway

Received: September 3, 2007; In Final Form: November 13, 2007

Starting from the phenomenological Bloembergen−Purcell−Pound equation a relation between magic-angle spinning (MAS) rate and spin diffusion is derived. The resulting model equation was fitted to observed spin diffusion versus MAS rate data obtained at 298 K on an high-density polyethylene sample, revealing a reduction in the effective spin diffusivity by (65 + 5)% when increasing the MAS rate from 2 to 12 kHz. The same model equation enabled the rigid-lattice diffusivity to be estimated and was found to be only slightly higher, by approximately 10%, compared to the spin diffusivity observed at the lowest MAS rate applied (2 kHz). Moreover, the model equation predicts a reduction in the effective spin diffusivity by more than 90% when increasing the MAS rate to more than 30 kHz.

Introduction

Solid-state NMR has been widely applied to explore the domain structure and the morphology of polymers. Using the SciFinder Scholar software, more than 1000 references were found containing the concepts morphology, polymer, and NMR. To obtain information regarding morphology and domain structure by solid-state NMR, the magnetization within a certain domain may be monitored as a function of diffusion time ("diffusion profile") by applying various magnetization transfer techniques (transfer of magnetization between phases/domains).[1−4] By model-fitting the initial part of this diffusion profile (initial rate approximation) or by fitting the complete diffusion profile (at all diffusion times) to an analytical solution of the diffusion equation (as derived from a solution of Fick's diffusion equation under proper initial conditions and spatial constraints),[1,4−7] structural information regarding spatial heterogeneities in a broad range of dimensions ranging from 0.1 to about 200 nm may be obtained. However, no matter what kind of method is employed, reliable spin diffusion coefficients for the respective domains are needed to obtain quantitative information regarding domain sizes.

In routine solid-state NMR, the use of magic-angle spinning (MAS) has proven to be crucial when probing molecular structure. For rare nuclei like ^{13}C, MAS mainly averages out chemical shift anisotropy of the rare spins and reduces the ^{1}H−^{13}C dipolar interaction. This, in turn leads to a significant enhancement in spectral resolution, which would otherwise result in a rather broad and featureless spectrum. Many of the above-mentioned NMR publications involve a combination of cross polarization (CP) and MAS (with the objective to discriminate between the different phase components) and make implicitly use of spin diffusion coefficients (D) as derived from static experiments or theoretical calculation without considering the effect of MAS.[8−10] Because the spin diffusivity also depends on the dipolar interaction, it will consequently depend on the MAS rate as well.[11−17] The influence of MAS rate on spin diffusivity has been well documented from both ^{1}H-, ^{13}C- and ^{15}N NMR[16,17] experiments. Various recoupling pulse sequences may be applied to counterbalance the decreasing spin diffusivity caused by MAS.[16] Also, analytical calculations as well as numerical simulations have been presented to obtain internuclear distances from proton-driven spin-diffusion experiments under MAS.[17] To improve the reliability of such diffusion-dependent parameters, a relation between diffusivity and MAS rate needs to be established.

In 1993, Schmidt-Rohr et al. reported on a correlation between line width and spin diffusivity[4] and noticed that an overestimation of the residual dipolar coupling may result due to spectral overlap. Later, Mellinger et al. showed[18] that for mobile polymers the spin diffusivity could be correlated to the effective spin−spin relaxation rate [$(T_2^*)^{-1}$]. Cherry[19] applied this method successfully on polymer membranes using both double quantum (DQ) filter and spin-diffusion MAS. Also, Jia et al.[20] reported on a general method based on intramolecular spin diffusion to measure and calculate the spin-diffusion coefficient in amorphous polymers and blends under moderate MAS speeds (3.5−4.5 kHz). Furthermore, Reichert et al.[21] and Krushelnitsky and co-workers[22] studied the influence of MAS on spin diffusion among ^{13}C− and ^{15}N nuclei by employing one-dimensional solid-state MAS exchange experiments.

Additionally, it is known that the sample temperature increases markedly with increasing MAS rate and thus affects the spin diffusivity as well. Therefore, to study the influence of MAS rate on spin diffusivity the actual sample temperature under the specified MAS conditions needs to be known. To the best of our knowledge, this change of sample temperature under MAS has seldom been critically corrected when considering ^{1}H spin-diffusion measurements. Because of the increasing interest in spin-diffusion experiments under high MAS frequency, we therefore need to know how the MAS rate affects

* Corresponding authors. E-mail: (E.W.H.) eddywh@kjemi.uio.no; (Q.C.) qchen@ecnu.edu.cn; (L.Z.) lili.zhang@kjemi.uio.no.
† East China Normal University.
‡ University of Oslo.

10.1021/jp077067u CCC: $40.75
Published on Web 01/23/2008

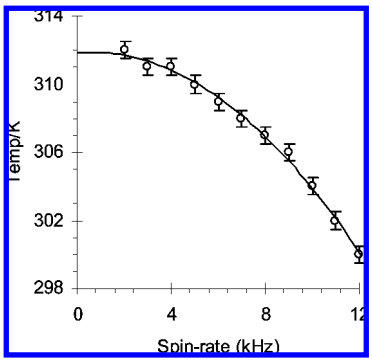

Figure 1. Variation of the sample (PE) temperature as a function of MAS rate, as determined by the chemical shift of ^{207}Pb in $Pb(NO_3)_2$, which defines the internal "NMR thermometer". The solid curve represents a second-order polynomial fit: $T = a_0 + a_1\nu_R + a_2\nu_R^2$ with $a_0 = 311.9$, $a_1 = 0.102$, and $a_2 = 0.0897$. T is the temperature (K) and ν_R is the MAS-frequency (kHz).

spin diffusivity under constant sample temperature to explore the relationship between MAS rate and spin diffusivity.

In this work, we will report on a series of spin-diffusion experiments on a high-density polyethylene (HDPE) sample performed at the same sample temperature (by correcting the temperature increase due to MAS) using a "dipolar filter"[1,23] combined with CP/MAS. A rather general equation relating spin diffusion to MAS rate will be presented based on a simple phenomenological consideration.

Experimental Section

Material. The HDPE powder sample was obtained from Sigma-Aldrich Company (CAS-9002-88-4) with $M_w = 3 \times 10^6 \sim 6 \times 10^6$ g/mol. It was melted at 160 °C and subsequently quenched in liquid nitrogen to produce a material with a reproducible thermal history, possessing a relatively small degree of crystallinity of (58.7 ± 0.3)% (as determined by ^{1}H−FID analysis[24a]) compared to an isothermally crystallized material. The molecular weight M_w was not known. However, M_w has little influence on the morphology, except for ultrahigh molecular weight PE samples.

NMR Measurement. All NMR experiments were performed on a Bruker DSX 300 spectrometer operating at a proton frequency of 300.13 MHz with a MAS double-resonance probe. All chemical shifts are referenced to tetramethylsilane with the orthorhombic crystalline peak possessing a chemical shift of $\delta = 32.9$ ppm.

The remarkable temperature sensitivity of the ^{207}Pb chemical shift in solid $Pb(NO_3)_2$ provides an excellent internal thermometer for solid-state MAS NMR,[24b] and enables the temperature of the PE sample to be probed as a function of the MAS rate with reasonable accuracy (±0.5 K). The results are summarized in Figure 1 in which the solid curve represents a second order polynomial fit to the observed data. By monitoring the ^{207}Pb chemical shift of $Pb(NO_3)_2$, we thus performed all spin-diffusion measurements presented in this work at the same sample temperature by adjusting the temperature of the bearing gas.

The generalized pulse sequence used in the spin-diffusion experiments is shown in Figure 2 and was composed of a dipolar filter followed by a spin-diffusion window of duration τ_m prior to the CP term. The dipolar filter refocused the dipolar coupling and chemical shift of the mobile protons while the rigid phase signal was depleted due to its much stronger dipolar−dipolar coupling. This was accomplished by using a time delay of 9 μs between pulses in the "filter part" of the pulse sequence. The 90° proton radio frequency pulse was set to 2.6 μs with a cross-

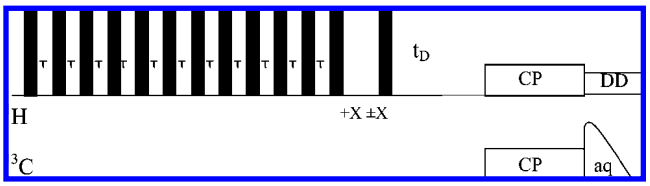

Figure 2. Schematic view of the pulse sequence applied to probe the spin diffusivity in PE. The first 12 proton pulses represent the "dipolar filter", which eliminates the magnetization within the crystalline phase (C) and leaves the amorphous phase (A) magnetization free to diffuse into the crystalline phase C. The magnetization present at the end of the evolution period was stored alternately along the $-z$ and $+z$ directions to minimize T_1 effects. CP is a short hand notation for cross-polarization.

polarization time of 1 ms. A total of 256 scans were accumulated with a repetition time of 5 s between successive scans.

We will assume that the spin diffusion takes place in a heterogeneous system possessing a lamellar morphology with magnetization diffusing from the amorphous region (A) and into a finite sink, representing the crystalline region C. Hence, a potential interface region located between the two former phases is neglected (this will be commented on in a later section). Hence, the magnetization transfer can be modeled analytically by solving the diffusion equation under proper initial- and constraint conditions, i.e., by considering a simple two-phase system under diffusion exchange. In short, the initial magnetization within the rigid phase C can be monitored as a function of diffusion time, or mixing time t_D as it diffuses from the mobile phase A and into the rigid phase

Theory. When considering dipole−dipole interacting proton nuclei and its effect on T_2, we may refer to the well-known Bloembergen−Purcell−Pound (BPP) equation[25]

$$\frac{1}{T_2} = \frac{2}{3} M_2^0(H)\left[3\tau + \frac{5\tau}{1+\omega^2\tau^2} + \frac{2\tau}{1+4\omega^2\tau^2}\right] \qquad (1)$$

where $M_2^0(H)$ is a constant derived from purely geometric considerations and denoted the proton rigid-lattice second moment. The parameter τ defines the time scale of the molecular dynamics and is denoted the correlation time. In general, the molecular dynamics within a system is seldom characterized by a single correlation time τ; often a distribution of correlation times has to be invoked. However, in this work we will use a rather simplified description based on an average molecular correlation time $\tau = \tau_{av}$. Also, we will assume phases A and C to be homogeneous in such a way that they are characterized by a single correlation time and a single diffusivity throughout their respective regions.

Equation 1 is strictly valid for fast motion on the NMR time scale, that is, for liquids ($\omega\tau \ll 1$). For solids, however, $\omega\tau$ may be much larger than 1, and eq 1 breaks down. In this case, the motional characteristics are better described by the following equation:[25−27]

$$\tau = \alpha \frac{1}{\sqrt{M_2(H)}} \tan\left[\frac{\pi}{2}\frac{M_2(H)}{M_2^0(H)}\right] \qquad (2a)$$

where $M_2(H)$ is the second moment of the proton absorption curve, and α is an adjustable parameter close to 1. Alternatively, in case the line shape does not change with MAS rate, the proton second moment $M_2(H)$ may be replaced by the proton line width $\Delta(H)$ that reads as follows:[27]

$$\tau = \beta \frac{1}{\Delta(H)} \tan\left[\frac{\pi}{2}\frac{\Delta^2(H)}{\Delta_0^2(H)}\right] \tag{2b}$$

where $\Delta_0(H)$ represents the rigid-lattice line width, and β is a constant. Notably, as $M_2(H)$ (or $\Delta(H)$) approaches its rigid-lattice limit $M_2^0(H)$ (or $\Delta_0(H)$), the correlation time τ becomes infinite, that is, the molecular traffic slows down dramatically. However, at room temperature a significant motional activity exists.

For purely dipolar spin interactions, the spin diffusivity D can be related to the proton second moment $M_2(H)$ of the NMR absorption line according to the following:[28]

$$D = k_0\langle r^2\rangle\sqrt{M_2(H)} \text{ and } D_0 = k_0\langle r^2\rangle\sqrt{M_2^0(H)} \tag{3}$$

where $<r^2>$ is the mean square distance between the nearest spins and k_0 is a constant. Inserting eq 3 into eq 2a gives

$$\tau = \alpha \frac{1}{\sqrt{M_2^0(H)}} \frac{D_0}{D} \tan\left[\frac{\pi}{2}\frac{D^2}{{D_0}^2}\right] \tag{4}$$

where D_0 defines the rigid-lattice spin diffusivity within the crystalline region of the nonspinning sample.

Apparent Motional Characteristics during Sample Spinning (MAS). From an NMR point of view, we may associate a sample-spinning of frequency ν_R by an additional superposed motion of the nuclear spins, characterized by a correlation time $\tau_R = 1/2\pi\nu_R$. One then expects the frequency of the modulation to be given by an apparent frequency ν_{app}, which is the sum of the contributing frequencies ν_R and ν, i.e., $\nu_{app} = \nu_R + \nu$ where the latter defines the frequency of the thermally activated (Arrhenius) process represented by the correlation time τ (eqs 2 and 4). How will an external spinning of a sample at a certain temperature T affect $M_2(H)$, and hence D?

Because the "molecular" motion induced by the sample spinning is independent of the thermally activated molecular motion, we may introduce an apparent correlation time τ_{app}, which can be expressed by a so-called "parallel-τ model"

$$\frac{1}{\tau_{app}} = \frac{1}{\tau} + \frac{1}{\tau_R} = \frac{1}{\tau} + 2\pi\nu_R \tag{5}$$

Equation 5 was introduced and discussed by Barnaal et al. in their work on relaxation time in doped ice.[29] Its applicability was motivated by the observed ^{1}H NMR spectra in Figure 3A (acquired at different MAS rates) in which the line width $\Delta(H)$ was derived by model fitting each spectrum to a pseudo Voigt function (see legend to Figure 3) and subsequently inserted into eq 2b to estimate the apparent molecular correlation time τ_{app} (setting $\beta = 1$ and the rigid-lattice line width $\Delta_0(H) \approx 65$ kHz[30]) within the amorphous phase. As can be inferred from Figure 3B, a linear relation between $1/\tau_{app}$ and MAS rate (ν_R) is noticed, thus giving support for the applicability of eq 5. Moreover, the estimated overall molecular correlation time $\tau = 3.0 \times 10^{-7}$ s of the amorphous phase (extrapolated from the straight line in Figure 3B at $\nu_R = 0$) is in excellent agreement with the corresponding correlation time reported in the literature[30b] on a similar PE sample. Notably, if changing the parameter β and/or $\Delta_0(H)$ the main effect is to displace the line vertically. Hence, eq 4 can be written as

$$\tau_{app} = \alpha \frac{1}{\sqrt{{M_2}^0(H)}} \frac{D_0}{D(T,\upsilon_R)} \tan\left[\frac{\pi}{2}\frac{D(T,\upsilon_R)^2}{{D_0}^2}\right] \leftrightarrow \frac{1}{\tau_{app}} = \frac{\sqrt{M_2^0(H)}D(T,\upsilon_R)}{\alpha D_0 \tan\left[\frac{\pi}{2}\frac{D^2(T,\upsilon_R)}{{D_0}^2}\right]} \tag{6}$$

where the diffusivity D is a function of both the temperature (T) and sample spinning frequency (ν_R), that is, $D(T,\nu_R)$. Because T is kept constant in all experiments reported in this work, for simplicity we will omit T in all subsequent formulas. By inserting eq 6 into eq 5

$$2\pi\upsilon_R = \frac{\sqrt{M_2^0(H)}D(\upsilon_R)}{\alpha D_0 \tan\left[\frac{\pi}{2}\frac{D^2(\upsilon_R)}{{D_0}^2}\right]} - \frac{1}{\tau} \tag{7}$$

and noting that

$$\frac{D^2}{{D_0}^2} = \frac{D^2(\upsilon_R)}{{D_0}^2} = \left(\frac{D^2(\upsilon_R)}{D^2(\upsilon_R^m)}\frac{D^2(\upsilon_R^m)}{{D_0}^2}\right) = x^2\lambda^2 \tag{8}$$

where $D(\upsilon_R^m)$ represents the spin diffusivity at the minimum MAS rate ($\nu_R = \upsilon_R^m$) applied and λ is a constant, defined by the ratio of the spin diffusivities $D(\upsilon_R^m)$ and D_0. Likewise, the parameter x represents the ratio of the spin diffusivities at MAS rates ν_R and υ_R^m, respectively, that is, $x = D(\nu_R)/D(\nu_R{}^m)$. By inserting eq 8 into eq 7

$$2\pi\upsilon_R = \frac{x\sqrt{M_2^0(H)}}{\alpha \tan\left[\frac{\pi}{2}\lambda^2x^2\right]} - \frac{1}{\tau} \tag{9}$$

Because the term $1/\tau$ (defined by the intrinsic molecular mobility) is constant for a given T, it can be determined from eq 8 by noting that $x = 1$ for $\nu_R = \upsilon_R^m$, which results in the following and final relation between MAS rate and spin diffusivity:

$$2\pi(\upsilon_R - \upsilon_R^m) = \frac{\sqrt{M_2^0(H)}}{\alpha}\left\{\frac{x}{\tan\left[\frac{\pi}{2}\lambda^2x^2\right]} - \frac{1}{\tan\left[\frac{\pi}{2}\lambda^2\right]}\right\} \tag{10}$$

For simplicity, we will assume that our system can be approximated by a two-phase system A and B, which are themselves spatially homogeneous (possessing the same spin diffusivity and the same molecular motions within their respective regions). It then follows that the ratio k ($= D_A/D_C$) between the two regional spin diffusivities is constant and satisfies the inequality $0 < k < 1$. By defining the effective diffusivity D_{eff} according to[1]

$$\frac{1}{\sqrt{D_{eff}}} = \frac{1}{\sqrt{D_A}} + \frac{1}{\sqrt{D_C}} \tag{11a}$$

we obtain

$$D_{eff} = \frac{4k}{(1+\sqrt{k})^2} D_C \tag{11b}$$

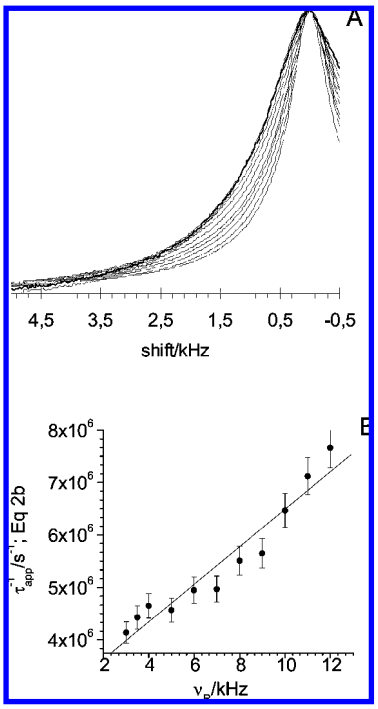

Figure 3. (A) ^{1}H NMR spectra (amorphous phase) acquired at different MAS rates ν_R (= 3, 3.5, 4, 5, 6, 7, 8, 9, 10, 11, and 12 kHz; from left to right). For visual purposes only, the left part of the symmetric amorphous peak is displayed. Each spectrum was fitted to a pseudo Voigt functions (V), defined by $V(\delta; \delta_C, \Delta, m) = I(m\ (2/\pi)(\Delta(H))/(4(\delta - \delta_C)^2 + \Delta(H)^2) + (1 - m)(4\ \ln\ 2)/\sqrt{\pi}\Delta\ \exp(-\sqrt{4\ln 2}/\Delta^2(H)(\delta - \delta_C)^2)$ where I defines the area of the peak and $\Delta(H)$ represents the width at half-height. Within experimental error, the adjustable parameter m was found to be independent of MAS rate and equal to 1 (Lorentzian curves). For illustration purposes, all spectra are plotted with the same height. (B) The apparent inverse correlation time $1/\tau_{app}$ (as derived from eq 2b by choosing $\beta = 1$ and $\Delta_0(H) = 65$ kHz) against MAS rate (ν_R).

At this point, it must be emphasized that we do not know whether the parameter k in eq 11b is constant and independent of MAS rate. Actually, it may well be that D_C and D_A behave differently with respect to MAS rate. This work is in progress and will be reported elsewhere. Of particular importance, our simplified model is one-dimensional and does not include molecular dynamics such as chain transport (chain diffusion). Thus, magnetization can be transported by chain diffusion even at room temperature. The chains in HDPE crystallites can move rather fast along the all-trans axis and thus decoupling a chain from its neighbors, whereby spin diffusion could be anisotropic, resulting in a spatial dependence of k. However, we emphasize that a main objective of this work is for the first time to justify the applicability of eq 10.

In a typical spin-diffusion experiment, we measure the signal intensity I of the crystalline phase against the square-root of diffusion time ($\sqrt{t_D}$). From these measurements, we can determine the characteristic time parameter $\sqrt{t_D^0}$, as illustrated in Figure 4, which is defined by the intersection point between the two straight lines $I = I_0$ (I_0 is equal to the constant magnetization obtained at long diffusion times, i.e., $t_D = \infty$; cf. dotted horizontal line in Figure 4) and the initial rate equation (cf. solid lines in Figure 4), and enables the average dimension ($<R>$) of a domain to be determined from eq 11c[1,31,32]

$$\langle R\rangle^2 = aD_{eff}t_D^0 \tag{11c}$$

where a is a constant depending on the morphology of the

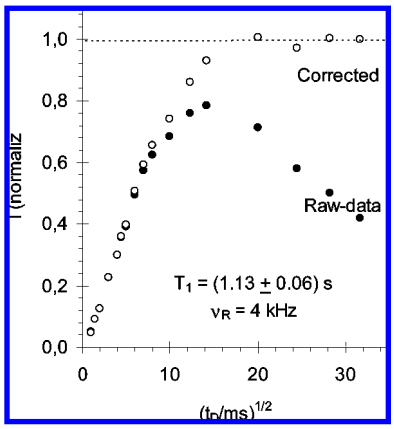

Figure 4. Signal intensity within the crystalline region of PE as a function of the square-root of diffusion time $\sqrt{t_D}$. The measurements were performed at 295 K using a MAS spin-rate of 4 kHz. Black circles are raw data and open circles represent corrected (for spin-lattice relaxation, see ref 1) data.

system.[31,32] Because the domain size $<R>$ must be independent of MAS rate, we obtain

$$\langle R^2\rangle = aD(\upsilon_R^A)t_D^0(\upsilon_R^A) = aD(\upsilon_R^B)t_D^0(\upsilon_R^B) = aD(\upsilon_R^m)t_D^0(\upsilon_R^m)$$

$$\leftrightarrow$$

$$x = \frac{D(\upsilon_R)}{D(\upsilon_R^m)} = \frac{t_D^0(\upsilon_R^m)}{t_D^0(\upsilon_R)} \tag{12}$$

where υ_R^A and υ_R^B represent two different MAS rates. Hence, we can easily determine x ($= t_D^0(\upsilon_R^m)/t_D^0(\upsilon_R)$) from the spin-diffusion experiments by applying eq 10

$$\frac{2\pi\upsilon_R - 2\pi\upsilon_R^m}{2\pi\upsilon_R^M - 2\pi\upsilon_R^m} =$$

$$F(x;\lambda) \leftrightarrow \upsilon_R = (\upsilon_R^M - \upsilon_R^m)\cdot F(x;\lambda) + \upsilon_R^m \tag{13a}$$

υ_R^M represent the highest (maximum) MAS frequency applied in the experiment, and

$$F(x;\lambda) = \left[\frac{x}{\tan\left[\frac{\pi}{2}\lambda^2x^2\right]} - \frac{1}{\tan\left[\frac{\pi}{2}\lambda^2\right]}\right] \tag{13b}$$

Results and Discussion

A spin-diffusion experiment performed on an HDPE sample at the smallest MAS rate ($\upsilon_R^m = 4$ kHz) is shown in Figure 4 by using the pulse sequence depicted in Figure 2. The significant deviation of the signal intensity from a constant value at $t_D >$ 200 ms originates from a spin−lattice (T_1) relaxation effect and was compensated for by multiplying the observed signal intensity by the term $\exp(t_D/T_1)$ in which T_1 was determined in an independent experiment: $T_{1H} = (1.14 \pm 0.06)$ s.[1] A corresponding T_1 correction was performed on all spin-diffusion data obtained. For clarity reasons, only four of these data sets are depicted in Figure 5.

It has recently been reported[33] that the signal intensity I as a function of the square root of spin-diffusion time $\sqrt{t_D}$ can be well approximated by a Boltzmann function

$$I(t_D) = a_2 + \frac{a_1 - a_2}{1 + \exp((\sqrt{t_D} - \sqrt{t_0})/\Delta)} \tag{14}$$

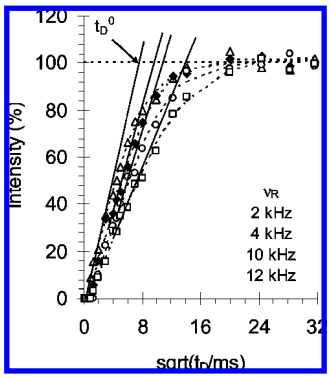

Figure 5. Signal intensity within the crystalline region of PE as a function of the square-root of diffusion time t_D determined at 4 different MAS rates ν_R. The measurements were performed at 295 K. The dotted curves represent model fits to a Boltzmann function (eq 15a), which enables the initial-rate approximation curve (solid lines) to be extracted. The dotted horizontal line represents the "limiting" signal intensity ($I = a = 100\%$) at long diffusion times t_D. The intersection point between these two lines defines the spin-diffusion time t_D^0.

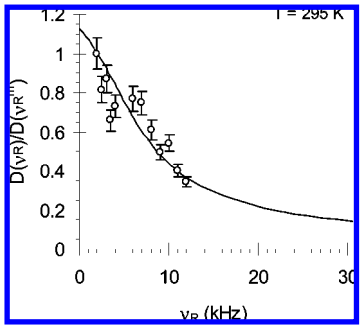

Figure 6. Spin diffusivity (within the crystalline region of a PE sample) as a function of MAS rate. The solid curve represents model fit (eq 13) to the observed data. The relative error of the spin diffusivity was estimated to be 8% and is illustrated by error bars. See text for further details.

where a_1, a_2, $\sqrt{t_0}$, and Δ represent adjustable model parameters. At the very beginning of the diffusion process ($t_D < 0.5$ ms), all diffusion curves reveal only a modest increase in intensity with diffusion time after which a significant and abrupt increase in intensity is observed, indicating the existence of an interfacial region between the amorphous and the crystalline regions. If approximating the spin diffusivity within this region to be the same as the spin diffusivity within the crystalline region, we find (Figure 5) that this "intermediate phase" has a dimension (in the direction of diffusion) that is less than 10% of the corresponding dimension within the crystalline region. On this ground, we approximate our system to be composed of only two phases: an amorphous and a crystalline phase, respectively.

A first attempt to fit eq 14 to all the experimental spin-diffusion curves (Figure 5) revealed that all three parameters a_1, a_2, and $\sqrt{t_0}$ were constant and independent of the MAS rate (ν_R). Only the width parameter Δ varied with ν_R. Moreover, within experimental error, a_1 was found to be equal to a_2, suggesting that the signal intensity I as a function of the square root of spin-diffusion time $\sqrt{t_D}$ can be well approximated by a simpler version of the Boltzmann function, eq 15a:

$$I(t_D) = a - \frac{2a}{1 + \exp((\sqrt{t_D} - \sqrt{t_0})/\Delta)} \qquad (15a)$$

with $a = 102 \pm 6$, $\sqrt{t_0} = (0.1 \pm 0.6)$ ms$^{1/2}$ and Δ being the

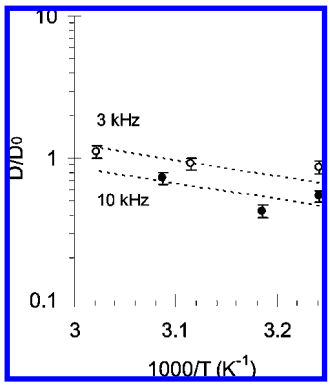

Figure 7. The spin diffusivity as a function of temperature at two different MAS rates of 3 and 10 kHz, respectively. The dotted curves represent model fits to an Arrhenius type of function $D = D_0 \exp(-\Delta E/RT)$ with $\Delta E = 12 \pm 5$ kJ/mol.

only MAS rate dependent parameter. From eq 15a, the initial rate equation can be easily derived (by differentiation) and reads

$$I_{IR}(t_D) = (a/2\Delta)\sqrt{t_D} - a\sqrt{t_0}/2\Delta \qquad (15b)$$

As already pointed out, this enables the important parameter $\sqrt{t_D^0}$ in eq 11b to be determined by setting $I_{IR}(t_D) = a$ (where a is equal to the constant magnetization obtained at long diffusion times ($t_D = \infty$; cf. Figure 4), that is

$$\sqrt{t_D^0} = 2\Delta + \sqrt{t_0} \qquad (15c)$$

Because Δ was found to be larger than 4 ms$^{1/2}$ and $\sqrt{t_0} = (0.1 \pm 0.6)$ ms$^{1/2}$, we may, within experimental error, approximate eq 15c by

$$\sqrt{t_D^0} = 2\Delta \qquad (15d)$$

Hence, the time parameter $\sqrt{t_D^0}$ is determined from Δ (eq 15d) by a simple nonlinear least-squares fit of eq 15a to the observed diffusion curve (cf. Figure 5).

The ratio $x = D(\nu_R)/D(\nu_R^m)$ between the spin diffusivities at any MAS rate ν_R and a reference MAS rate ν_R^m (minimum MAS rate applied in this work) was calculated from the experimentally determined spin-diffusion times $t_D^0(\upsilon_R)$ and $t_D^0(\upsilon_R^m)$ (eq 12) and is plotted against the MAS rate (Figure 6), which reveals a spin diffusivity that decreases by a factor of 4 when increasing the MAS rate from 2 to 16 kHz. This observed reduction of spin diffusivity with increasing MAS rate is of exactly the same order of magnitude (4−5) as reported recently by Krushelnitsky et al.[34] in their investigation on the proton spin diffusion between backbone ^{15}N nuclei in totally enriched protein.

The uncertainty in the sample temperature was estimated to be smaller than ±1 K. To estimate the propagating uncertainty in diffusivity due to this temperature uncertainty, the spin diffusivity was measured as a function of temperature for two different MAS rates of 3 and 10 kHz, respectively. The results are summarized in Figure 7 in which the dotted curves represent model fits to an Arrhenius type of function: $D = D_0 \exp(-\Delta E/RT)$ with $\Delta E = 12 \pm 5$ kJ/mol, resulting in an uncertainty in D of less than 2%. Hence, the overall error in D (Figure 6) originates mainly from the uncertainty in t_D (cf. Equation 12) and was found to be of the order of 8% (relative scale).

By fitting eq 13 to the observed MAS rate, the two adjustable parameters $x_0 = D(\upsilon_R^M)/D(\upsilon_R^m)$ and $\lambda = D(\upsilon_R^m)/D_0$ were determined to be 0.37 ± 0.02 and 0.92 + 0.08, respectively,

suggesting that the spin diffusivity reduces by (63 ± 5)% when increasing the MAS rate from 2 to 12 kHz, respectively. On the other hand, the rigid-lattice spin diffusivity D_0 is only marginally larger than the observed spin diffusivity at 2 kHz MAS rate. Referring to Figure 6, we find D_0 to be larger by only about 10%.

The error in x_0 and λ was determined by simulation, that is, by generating a series of 10 synthetic data sets. We started by calculating the spin diffusivity at 12 different MAS rates via eq 13 by using the model fitted parameters x_0 and λ. We then generated randomly 12 new diffusivity values by imposing a relative standard error of 8% in each diffusivity parameter. Each set of these synthetic data was subsequently fitted to eq 13, and the average of x_0 and λ was determined. The corresponding error in x_0 and λ was derived by traditional statistical procedures.

Conclusion

Starting from the phenomenological BPP equation, an expression relating the MAS rate ν_R to the spin diffusivity D is obtained, taking the form

$$\upsilon_R = (\upsilon_R^M - \upsilon_R^m)\cdot F(x;\lambda) + \upsilon_R^m$$

with

$$F(x;\lambda) = \left[x/\tan\left[\frac{\pi}{2}\lambda^2 x^2\right] - 1/\tan\left[\frac{\pi}{2}\lambda^2\right]\right],$$
$$x = D(\upsilon_R)/D(\upsilon_R^m),\ \lambda = D(\upsilon_R^m)/D_0$$

and υ_R^x representing the smaller (x = m) and higher (x = M) applied MAS rates, respectively. D_0 is the rigid−lattice spin diffusivity.

From model-fitting, the rigid-lattice diffusivity was estimated and found to be only slightly larger (by approximately 10%) compared to the spin diffusivity at the lowest MAS rate applied (2 kHz). Moreover, a reduction in spin diffusivity by nearly 90% was estimated when increasing the MAS rate to more than 30 kHz.

In short, we have demonstrated that the MAS rate has a marked influence on the spin diffusivity, and as a consequence great care must be taken when aiming at quantifying domain sizes from such spin-diffusion measurements, in particular at high MAS rates. Actually, using spin diffusivities obtained from static NMR measurements to determine the domain size from spin-diffusion measurements at high MAS rates (>10 kHz) may lead to a significant error in estimated domain sizes by more than 50%.

Acknowledgment. E.W. Hansen is obliged to UiO for economical support in preparing this manuscript during his visit at the Key Laboratory for Optics and Magnetic Resonance Spectroscopy, East China Normal University, ECNU in Shanghai, China. This work is also supported by the project of NSFC (No. 20474019) and by Program for Innovative Research Team in University.

References and Notes

(1) Schmidt-Rohr, K.; Spiess, H. W. *Multidimensional Solid-State NMR and Polymers*; Academic Press: London, 1994.
(2) Blümich, B. *NMR Imaging of Materials*: Clarendon Press: Oxford, 2000.
(3) (a) Demco, D. E.; Blümich, B. *Concepts Magn. Reson., Part I* **2000**, *12*, 188. (b) Demco, D. E.; Blümich, B. *Concepts Magn. Reson., Part II* **2000**, *12*, 269.
(4) Clauss, J.; Schmidt-Rohr, K.; Spiess, H. W. *Acta Polym.* **1993**, *44*, 1.
(5) Buda, A.; Demco, D. E.; Bertmer, M.; Blümich, B.; Litvinov, V. M.; Penning, J. P. *J. Phys. Chem. B* **2003**, *107*, 5357.
(6) VanderHart, D. L.; McFadden, G. B. *Solid State Nucl. Magn. Reson.* **1996**, *7*, 45.
(7) Wang, J. *J. Chem. Phys.* **1996**, *104*, 4850.
(8) Jack, K. S.; Wang, J.; Natansohn, A.; Register, R. A. *Macromolecules* **1998**, *31*, 3282.
(9) Silva, N. M.; Tavares, M. B.; Stejskal, E. O. *Macromolecules* **2000**, *33*, 115.
(10) Beshah, K.; Molnar, L. K. *Macromolecules* **2000**, *33*, 1036.
(11) Lowe, I. J. *Phys. Rev. Lett.* **1959**, *2*, 285.
(12) Andrew, E. R.; Bradbury, A.; Eades, R. G. *Nature.* **1959**, *183*, 1802.
(13) Kessemeier, H.; Norberg, R. E. *Phys. Rev.* **1967**, *155*, 321.
(14) Tekely, P.; Palmas, P.; Canet, D. *J. Magn. Reson., Ser. A* **1994**, *107*, 129.
(15) Neagu, C.; Puskas, J. E.; Singh, M. A.; Natansohn, A. *Macromolecules* **2000**, *33*, 5976.
(16) Alonso, B.; Massiot, D. *J. Magn. Reson.* **2003**, *163*, 347.
(17) Grommek, A.; Meier, B. H.; Ernst, M. *Chem. Phys. Lett.* **2006**, *427*, 404.
(18) Mellinger, F.; Wilhelm, M.; Spiess, H. W. *Macromolecules* **1999**, *32*, 4686.
(19) Cherry, B. R.; Fujimoto, C. H.; Cornelius, C. J.; Alam, T. M. *Macromolecules* **2005**, *38*, 1201.
(20) Jia, X.; Wolak, J.; Wang, X.; White, J. L. *Macromolecules* **2003**, *36*, 712.
(21) Reichert, D.; Bonagamba, T. J.; Schmidt-Rohr, K. *J. Magn. Reson.* **2001**, *151*, 129.
(22) Krushelnitsky, A.; Bräuniger, T.; Reichert, D. *J. Magn. Reson.* **2006**, *182*, 339.
(23) Cheng, J.; Fone, M.; Reddy, V. N.; Schwartz, K. B.; Fisher, H. P.; Wunderlich, B. *J. Polym. Sci., Part B: Polym. Phys.* **1994**, *32*, 2969.
(24) (a) Hansen, E. W.; Kristiansen, P. E.; Pedersen, B. *J. Phys. Chem. B* **1998**, *102*, 5444. (b) Bielecki, A.; Burum, D. P. *J. Magn. Reson.* **1995**, *116*, 215.
(25) Bloembergen, N.; Purcell, E.; Pound. R. V. *Phys. Rev.* **1948**, *73*, 679.
(26) Gutowski, H. S.; Pake. G. E. *J. Chem. Phys.* **1950**, *18*, 162.
(27) Abragam A. *The Principles of Nuclear Magnetism*; Clarendon Press: Oxford, 1961.
(28) Demco, D. E.; Johanson, A.; Tegenfeldt, J. *Solid State Nucl. Magn. Reson.* **1995**, *4*, 13 and references therein.
(29) Barnaal, D.; Kopp, M.; Lowe, I. J. *J. Chem. Phys.* **1976**, *65*, 5495.
(30) Packer, K. J.; Pope, J. M.; Yeung, R. R.; Cudby, M. E. A. *J. Polym. Sci., Polym. Phys Ed.* **1984**, *22*, 589.
(31) Kristiansen, P. E.; Hansen, E. W.; Pedersen, B. *J. Phys. Chem. B* **1999**, *103*, 3552.
(32) VanderHart, D. L. *Makromol. Chem., Macromol. Symp.* **1990**, *34*, 125.
(33) Havens, J. R.; VanderHart, D. L. *Macromolecules* **1985**, *18*, 1663.
(34) Zhang, L; Chen, Q; Hansen, E. W. *Macromol. Chem. Phys.* **2005**, *206*, 246.
(35) Kolodziejski, W.; Klinowski, J. *Chem. Rev.* **2002**, *102*, 613.